OBLIQUE MAGNETIC FIELDS AND THE ROLE OF FRAME DRAGGING NEAR A ROTATING BLACK HOLE

VLADIMÍR KARAS*, ONDŘEJ KOPÁČEK, DEVAKY KUNNERIATH,
JAROSLAV HAMERSKÝ

Astronomical Institute, Academy of Sciences, Boční II 1401, CZ-14000 Prague, Czech Republic

* corresponding author: vladimir.karas@cuni.cz

ABSTRACT. Magnetic null points can develop near the ergosphere boundary of a rotating black hole due to the combined effects of a strong gravitational field and the frame-dragging mechanism. The induced electric component does not vanish, and an efficient process of particle acceleration can occur. Furthermore, the effect of the imposed (weak) magnetic field can trigger the onset of chaos. The model set-up appears to be relevant for low-accretion-rate nuclei of some galaxies which exhibit episodic accretion events (such as the Milky Way's supermassive black hole) embedded in a large-scale magnetic field of external origin. We review our recent results and we give additional context for future work focused on the role of gravito-magnetic effects caused by the rotation of the black hole. While the test motion is strictly regular in the classical black hole space-time, with and without the effects of rotation or an electric charge, gravitational perturbations and imposed external electromagnetic fields may lead to chaos.

KEYWORDS: accretion; black holes; gravitation; magnetic fields.

1. INTRODUCTION

Cosmic black holes can act as agents of acceleration to very high energies of electrically charged particles in their immediate vicinity. At the same time, the motion of particles can exhibit a transition from regular to chaotic motion. In this overview, we describe the properties of a system consisting of a rotating black hole immersed in a large-scale magnetic field, i.e., an external (weak) field that is organized on length-scales exceeding the gravitational radius of the black hole, $R_{\rm g} \equiv GM_\bullet/c^2 \sim 1.5 \times 10^{13}\, M_8$ cm ($M_8 \equiv M_\bullet/10^8 M_\odot$, where $M_\bullet$ denotes the mass of the black hole). Electrically charged particles in the immediate neighborhood of the horizon are influenced by strong gravity acting together with magnetic and induced electric components.

We relax several constraints which were often imposed in previous works: the magnetic field does not have to share a common symmetry axis with the spin of the black hole. They can be inclined with respect to each other, thus violating axial symmetry. Also, the black hole does not have to remain at rest but it can instead perform a fast translational motion together with rotation. We demonstrate that the generalization brings new effects. Starting from uniform electro-vacuum fields in the curved spacetime, we find separatrices and identify magnetic neutral points forming in certain circumstances. We suggest that these structures can represent signatures of magnetic reconnection triggered by frame-dragging effects in the ergosphere. We further investigate the motion of charged particles in these black hole magnetospheres. We concentrate on the transition from regular motion

to chaos, and in this context we explore the characteristics of chaos in relativity. We apply recurrence plots as a suitable technique for quantifying the degree of chaoticness near a black hole.

Various parts of the scientific content of the present summary have been published in [27–29, 36] and in a PhD thesis [33]. An investigation of the particle motion in the astrophysical corona was preceded by a study of the topology of off-equatorial potential lobes presented in [38]. The charged particle motion in such lobes was also discussed in [37]. Initial steps in the investigation of electromagnetic fields around a drifting Kerr black hole were described in [32]. Here we bring together various aspects of the motion in the context of weakly magnetised black holes and, in the last section, we present the outlook and future prospects for our research line, together with open questions.

2. MOTIVATION FOR MAGNETIC NEUTRAL POINTS AS A TRIGGER OF PARTICLE ACCELERATION

Observations of microquasars, pulsars and gamma-ray bursts indicate that astrophysical jets play an important role almost everywhere, i.e., in various kinds of compact objects, ranging from stellar-mass black holes to supermassive black holes in active galactic nuclei (AGNs) and also in the starving supermassive black hole in the center of the Milky Way [43]. There is plenty of observational evidence suggesting that the initial acceleration of jets takes place very near black holes (and other compact objects) and that it proceeds via electromagnetic forces. Jets and accretion disks
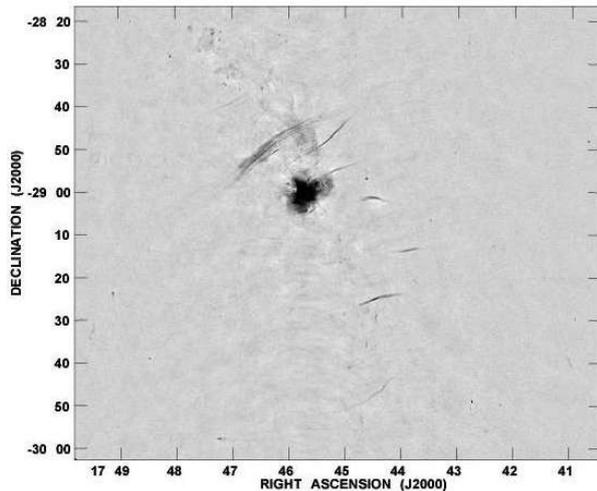
FIGURE 1. Tentative motivation for studying the effects of black holes embedded within organised (coherent) magnetic fields of external origin: The central region of the Milky Way is penetrated by narrow Non-Thermal Filaments (NTFs) which may suggest the presence of large-scale magnetic fields. In these regions the strength of the ordered magnetic field can approach $\approx 1\,\mathrm{mG}$. The length of the NTFs reaches tens of parsecs. The inner region of the Galactic center $0.8° \times 1.0°$ is shown at wavelength $90\,\mathrm{cm}$ ($330\,\mathrm{MHz}$; image taken by the Very Large Array (VLA); figure credits: [44, 55]).

in the vicinity of compact objects probably create a magnetically driven symbiotic system [17].

The current promising model of the dynamics (i.e. launching, accelerating, and collimating) of astrophysical jets is based on magnetohydrodynamics (MHD). The results of simulations employing general relativistic MHD equations [42] correlate with observations of M87 [26], where the formation and the collimation of the jet were analyzed.

Moreover, the 3D relativistic MHD simulations carried out by [22] demonstrate the essential role played by the accretion disk's coronae in the collimation and acceleration of jets. Indeed the dominant force accelerating the matter outward in a given numerical model originates from coronal pressure. Regions above and below the equatorial plane become dominated by the magnetic pressure, and large-scale magnetic fields may also develop by the dynamo action.

A recent relativistic (numerical) study by [61] reveals the formation of the ordered jet-like structure of an ultra-strong magnetic field in the merger of binary neutron stars. Such a system might therefore serve as an astrophysical engine for the observed short gamma ray bursts.

Small-scale (turbulent) magnetic fields have also been employed in accretion physics, where the magnetorotational instability (MRI) is believed to operate in accretion flows, generating the effective viscosity necessary for the accretion process [7]. Magnetic reconnection is likely to be responsible for the rapid

flares that are observed in X-rays. Finally, Faraday rotation measurements suggest that tangled magnetic fields are present in jets [10].

Observations of the Galactic center (GC) reveal the presence of another remarkable large-scale magnetic structure: Non-Thermal Filaments (NTFs). These primarily linear structures cross the Galactic plane, and their length reaches tens of parsecs while they are only tenths of a parsec wide. The strength of the magnetic field within the NTF may approach $\approx 1\,\mathrm{mG}$, while the typical interstellar value is $\approx 10\,\mu\mathrm{G}$ [44]. Initially, it was thought that NTFs trace the pervasive poloidal magnetic field present throughout the GC [54]. Later, however, it became apparent that the structure of the magnetic field in the central region of the Galaxy is more complex [18]. See, e.g., [44, 55] and Figure 1 for snapshots of the GC at $90\,\mathrm{cm}$ ($330\,\mathrm{MHz}$) that exhibit NTFs.

Overall, it is quite likely that electromagnetic mechanisms play a major role and operate near both supermassive black holes in quasars as well as stellar-mass black holes and neutron stars in accreting binary systems. In addition a faint magnetic field is present throughout the interstellar medium, and is locally intensified in NTFs.

3. ELECTRICALLY CHARGED PARTICLES NEAR A BLACK HOLE

3.1. ELECTRO-VACUUM FIELDS

A theoretical survey of the properties of vacuum electromagnetic (EM) fields may be regarded as the fundamental starting point for a study of the dynamics of diluted astrophysical environments. In the next stage we will consider the motion of non-interacting particles exposed to these fields. The structure of a particular astrophysically motivated EM field emerging in the vicinity of a rotating black hole has been studied in detail, see [11, 12, 33] and references therein. Subsequently we also discuss the motion of charged particles exposed to the field representing a special case of a general solution explored before. We concern ourselves primarily with the stable orbits occupying off-equatorial potential lobes. Particles on these orbits are relevant for a description of the astrophysical corona consisting of diluted plasma residing outside the equatorial plane in the inner parts of accreting black hole systems.

A gaseous corona is considered supposed to play a key role in the formation of he observed X-ray spectra of both active galactic nuclei (AGNs) and microquasars [15]. The power law component of the spectra is believed to result from the inverse Compton scattering of the thermal photons emitted in the inner parts of the disk. Relativistic electrons residing in the corona serve as scatterers in this process. Their dynamic properties (e.g., resonances) will therefore leave their imprint on the observed spectra.

The role of magnetic fields near strongly gravitating objects has been the subject of many investigations [60]. They are relevant for accretion disks that may be embedded in large-scale magnetic fields, for example when the accretion flow penetrates close to a neutron star [45, 51]. Outside the main body of the accretion disk, i.e., above and below the equatorial plane, the accreted material forms a highly diluted environment, a corona, where the density of the matter is low and the mean free path of the particles is large in comparison with the characteristic length-scale, i.e., the gravitational radius of the central body, $r = R_g$. The origin of the coronal flows and the relevant processes governing their structure are still unclear. In this context, we discuss the motion of electrically charged particles outside the equatorial plane.

3.2. Regular and chaotic dynamics

Accretion onto black holes and compact stars brings material into a zone of strong gravitational and electromagnetic fields. We study the dynamical properties of motion of electrically charged particles forming a highly diluted medium (a corona) in the regime of strong gravity and a large-scale (ordered) magnetic field.

We start our discussion from a system that allows regular motion, and then we focus on the onset of chaos. To this end, we investigate the case of a rotating black hole immersed in a weak, asymptotically uniform magnetic field. We also consider a magnetic star, approximated by the Schwarzschild metric and a test magnetic field of a rotating dipole. These are two model examples of systems permitting energetically bound, off-equatorial motion of matter confined to the halo lobes that encircle the central body. Our approach allows us to address the question of whether the spin parameter of the black hole plays any major role in determining the degree of chaoticness.

The two dynamic systems may be regarded as different instances of the originally integrable systems which were perturbed by the electromagnetic test field. Complete integrability of the geodesic motion of a free particle in Schwarzschild spacetime is easy to verify [52]. To some surprise, it was later found that also the free particle motion in Kerr spacetime and even the charged particle motion in Kerr-Newman is completely integrable [13] since the equations of motion are separable, is possible as there exists an additional integral of motion – Carter's constant $\mathcal{L}$. Trajectories found in such a system are purely regular.

In the non-integrable system, however, both regular and chaotic trajectories may coexist in the phase space. The standard method for a qualitative survey of non-linear dynamics is based on the construction of Poincaré surfaces of a section that allows us to discriminate visually between chaotic and regular regimes of motion.

However, quantifying chaos by Lyapunov Characteristic Exponents (LCEs), as its standard and commonly used indicator, becomes problematic in General Relativity (GR), because LCEs are not invariant under coordinate transformations. In addition, the usual method for computing LCEs involves evaluating the distances between the neighbouring trajectories, which becomes intricate in GR. Although there are operational workabouts to partially overcome these difficulties [68], the need for a consistent treatment is apparent. The geometrical approach suggested recently by [63] could eventually provide a covariant method or evaluating the Lyapunov spectra in GR.

In this context, we adopt a different tool to investigate the dynamic system — Recurrence Analysis [49]. To characterize the motion, we construct Recurrence Plots (RPs) and we compare them with Poincaré section surfaces. We describe the Recurrence Plots in terms of Recurrence Quantification Analysis (RQA; see Figure 10 below), which allows us to identify the transition between different dynamical regimes. We demonstrate that this new technique is able to detect the onset of chaos very efficiently, and to provide a quantitative measure of it. Chaos typically occurs when the conserved energy is raised to a sufficiently high level that allows the particles to traverse the equatorial plane. We find that the role of black-hole spin in setting the chaos is more complicated than was initially thought.

4. Near-horizon structure of oblique electromagnetic test fields: magnetic null points and layers

4.1. Effects of the Kerr metric on weak magnetic fields

In [33] we went through various issues concerning the structure of the electromagnetic field that arises from the interplay between the frame-dragging effect and the uniform magnetic field with general orientation with respect to the rotation axis of the Kerr source. We further generalized the model by allowing the black hole to move translationally in a general direction with respect to the magnetic background. Components of the electromagnetic tensor $F_{\mu\nu}$ describing the resulting field were given explicitly (in a symbolic way regarding their length) in terms of the former non-drifting solution. Special attention was paid to the comparison of various definitions of the electric/magnetic field. We also reviewed the construction of three distinct frames attached to the physical observers.

We have been interested in solutions describing an originally uniform magnetic field under the influence of the Kerr black hole (see Figures 2–3). Since the Kerr metric is asymptotically flat, this EM field reduces to the original homogeneous magnetic field in the asymptotic region. A test field solution of thys type was first given in [67] for the special case of perfect alignment of the asymptotically uniform magnetic field
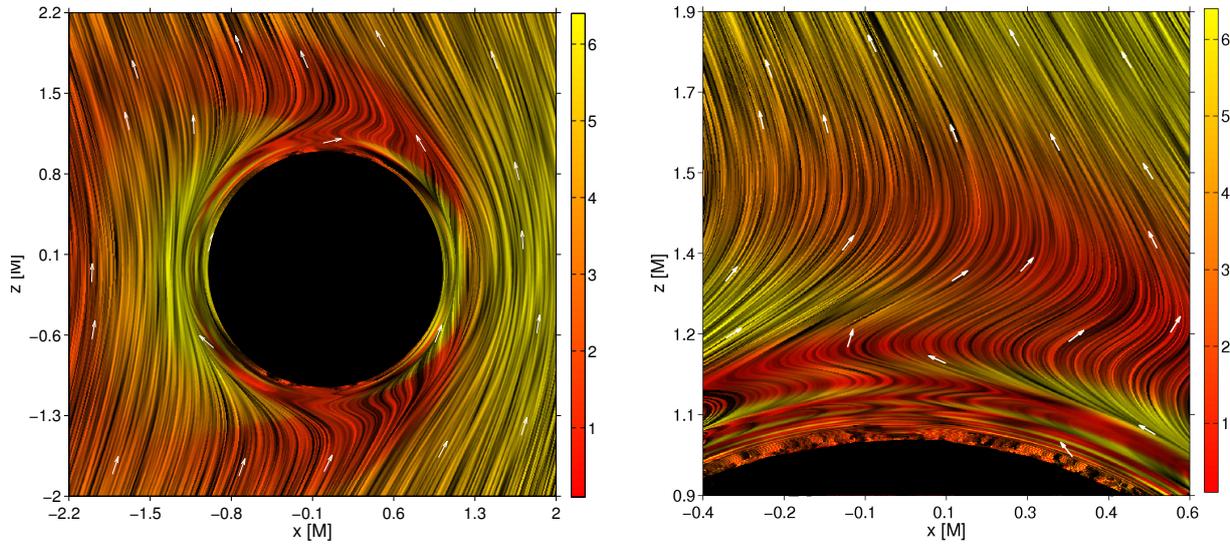
FIGURE 2. These plots cover the immediate vicinity of a rotating (Kerr) black hole (black circle), i.e. the region within and just outside of the ergosphere. Here, we show the drift-induced effects (i.e., the effects caused by the translation boost of the linear motion of the black hole) as well as the frame dragging effects (due to rotation) on the structure of the aligned magnetic field (extreme spin, $a = M$). Magnetic field lines are shown and their changing direction is indicated by arrows. The translational motion of the black hole is restricted to be parallel with the horizontal axis, $v_x = 0.5c$, $v_y = v_z = 0$. We observe a narrow front that develops above the horizon, where the field lines have a complex, multi-layered structure. The colour scale indicates the intensity of the field (in arbitrary units). See [33] for further details and references.
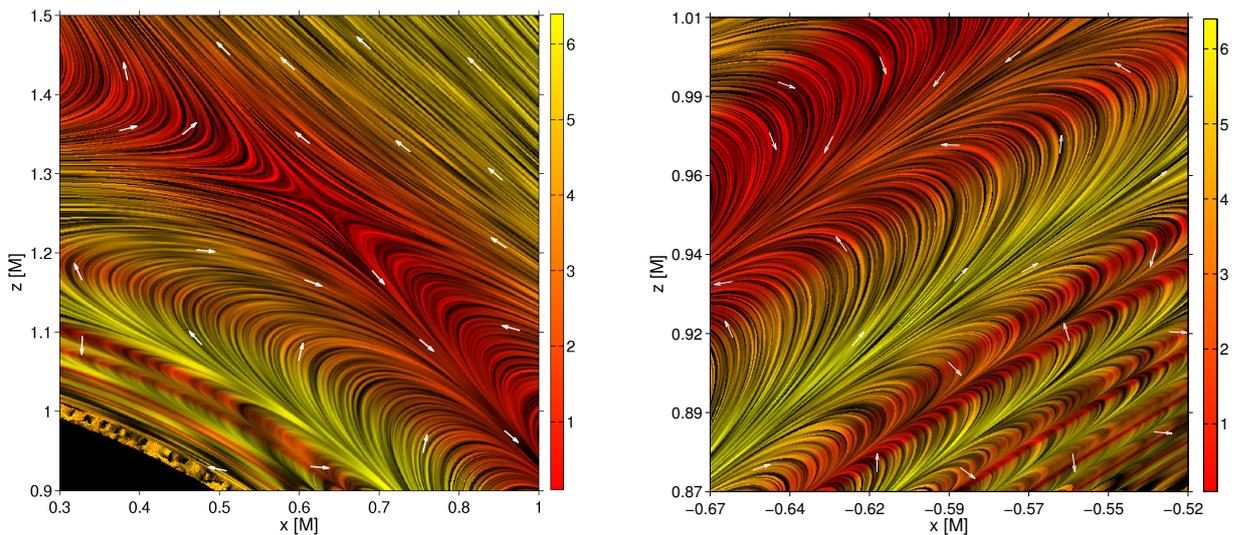
FIGURE 3. Effects of a linear translator boost of the rotating black hole acting on the structure of the aligned magnetic field. The field distortions increase profoundly in the case of extremely fast motion $v_x = 0.99c$. A neutral (null) point of the magnetic field occurs (left panel). We observe self-similar tightly folded layered structures which become considerably enhanced in comparison to the case of slower motion presented previously in Figure 2 (right panel).

with the symmetry axis. Using a different approach of Newman Penrose formalism, a more general solution for an arbitrary orientation of the asymptotic field was inferred by [11]. We departed from their solution to construct the EM field around the Kerr black hole which is drifting through the asymptotically uniform magnetic field.

By introducing the geometrized units ($G = c = k = k_C = 1$), the Kerr metric in Boyer-Lindquist coordinates $x^\mu = (t, r, \theta, \varphi)$ can be expressed in the following form [52]:

$$ds^2 = -\frac{\Delta}{\Sigma}[dt - a\sin\theta\, d\varphi]^2$$
$$+ \frac{\sin^2\theta}{\Sigma}\big[(r^2 + a^2)d\varphi - a\, dt\big]^2 + \frac{\Sigma}{\Delta}\, dr^2 + \Sigma\, d\theta^2, \quad (1)$$

where

$$\Delta \equiv r^2 - 2Mr + a^2, \quad \Sigma \equiv r^2 + a^2\cos^2\theta, \quad (2)$$

while a stands for the dimensionless spin of the black hole ($|a| \leq 1$), and $M \equiv M_\bullet$ stands for its mass. In our work we assume that the metric terms and the corresponding gravitational field are not perturbed, i.e., the gravitational influence of the electromagnetic field is assumed to be negligible.

We compared several possible definitions of electric and magnetic field vectors. First we remained in the coordinate basis and defined *coordinate, physical, renormalized* and *asymptotically motivated (AMO)* components of the fields. These differ in their behaviour close to the horizon of the black hole and appear useful when exploring the field structures, but they allow for a clear physical interpretation only in the asymptotical region. A consistent definition of the electric and magnetic fields should, however, provide a natural physical interpretation of the observables measured by certain physical observer at any distance from the center. We let such an observer with four-velocity u^μ equipped with the orthonormal tetrad $e_{(\alpha)}{}^\mu$ measure the Lorentz force using his tetrad basis. Tetrad components of the vector fields defining the desired lines of force are given as the spatial part of the projection

$$B^{(i)} = B_{(i)} = -e^{(i)}{}_\mu \,{}^*F^\mu{}_\nu u^\nu$$
$$= -e_{(i)}{}^\mu \,{}^*F_{\mu\nu} e^\nu{}_{(t)} = -{}^*F_{(i)(t)}, \quad (3)$$
$$E^{(i)} = E_{(i)} = e^{(i)}{}_\mu F^\mu{}_\nu u^\nu$$
$$= e_{(i)}{}^\mu F_{\mu\nu} e^\nu{}_{(t)} = F_{(i)(t)}, \quad (4)$$

where $e^{(\alpha)}{}_\mu$ are 1-forms dual to the tetrad vectors $e^\mu{}_{(\alpha)}$.

We also discuss the choice of the tetrad in detail [33]. Namely we employed the standard ZAMO (zero angular momentum observer) tetrad and the tetrad of the observer who is freely falling from rest at infinity (FFOFI). In the equatorial plane we also used the astrophysically relevant tetrad attached to the circular

Keplerian observer above the marginally stable orbit and freely inspiralling to the horizon under this orbit (keeping the Keplerian angular momentum and energy of the innermost orbit). However, in this text we only present the field structures measured by FFOFI.

Before exploring the rich structures arising from the drift and oblique background field we first revisited the issue of the expulsion of the aligned magnetic field out of the horizon of the extremal Kerr black hole (Meissner effect). Although the effect itself has already been discussed extensively in the literature, its origin has not been fully understood and the investigation has continued in very recent papers in the context of the original motivation for astrophysical jets from magnetised black holes [56] and even for a novel and quite surprising relation of the phenomenon to the problem of entanglement [57]. Nevertheless, the issues of non-axisymmetric configurations remain largely unexplored.

The continued interest in the black-hole Meissner effect is understandable: it has been argued that the impact of the effects can lead to quenching astrophysical jets, so it is important to understand what causes the effect, how it operates in astrophysically realistic environments, and how it could be evaded. We do not solve the problem in our present paper; here we concentrate on the observer aspect of the problem instead. By comparing alternative definitions of the magnetic vector field combined with the choice of the four-velocity profiles, we came to the conclusion that:

(1.) the Meissner effect is observer dependent;

(2.) some definitions of the field lines do not fit well into the Boyer-Lindquist coordinate system since they artificially amplify the effect of the coordinate singularity at the horizon.

Namely we observed that in the ZAMO tetrad the field does not exhibit the Meissner effect, while in the FFOFI frame the field is expelled. However, in the renormalized field components expulsion is observed both for ZAMO and for FFOFI test charges. In coordinate components the Meissner effect also appears, but we decided not to use them because the coordinate basis is not normalized, which causes artificial deformation of the field lines. On the other hand, the properly normalized physical components appear problematic since they amplify the effect of the coordinate singularity at the horizon, as mentioned above. We found them to be quite inconvenient for use in the Boyer-Lindquist coordinate system (especially in the region very close to the horizon). Asymptotically-motivated (AMO) components, which are *observer independent* as they reflect the $F_{\mu\nu}$ components directly, were also employed and the resulting magnetic lines of force were identified with the section of the surfaces of the constant magnetic flux, which represent yet another way to display the field. We note that in the FFOFI frame both magnetic and electric fields are expelled out of the horizon in the case of extremal spin.
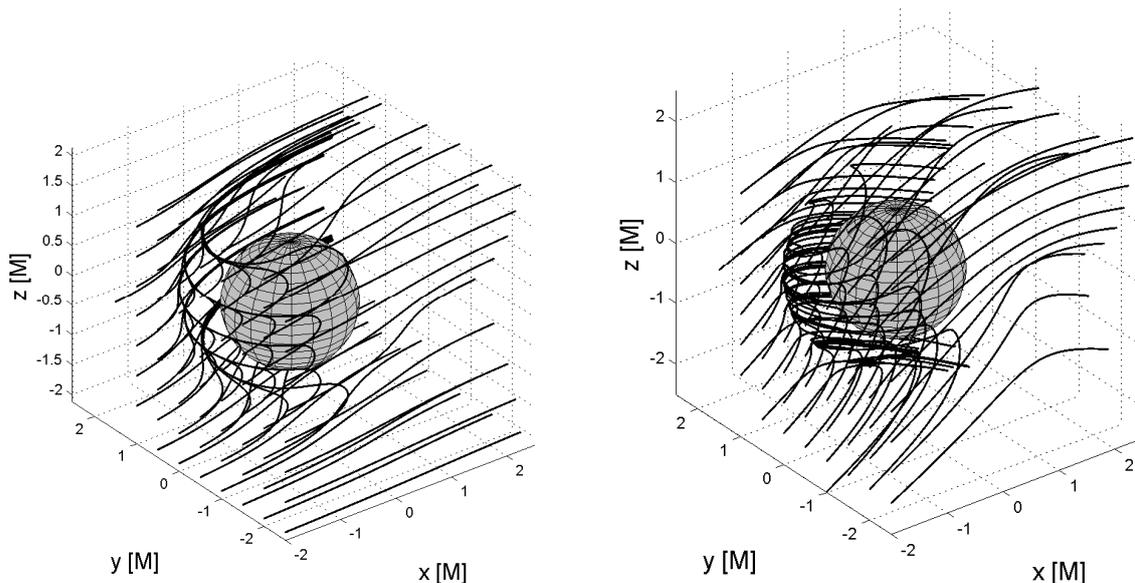
FIGURE 4. The extreme Kerr black hole which rotates along the z-axis is immersed in the perpendicular magnetic field $B_x > 0$. The left panel shows the situation with zero drift speed while in the right panel we observe the impact that the drift motion of the black hole along the z-axis ($v_z = 0.7c$) has upon the field structure.
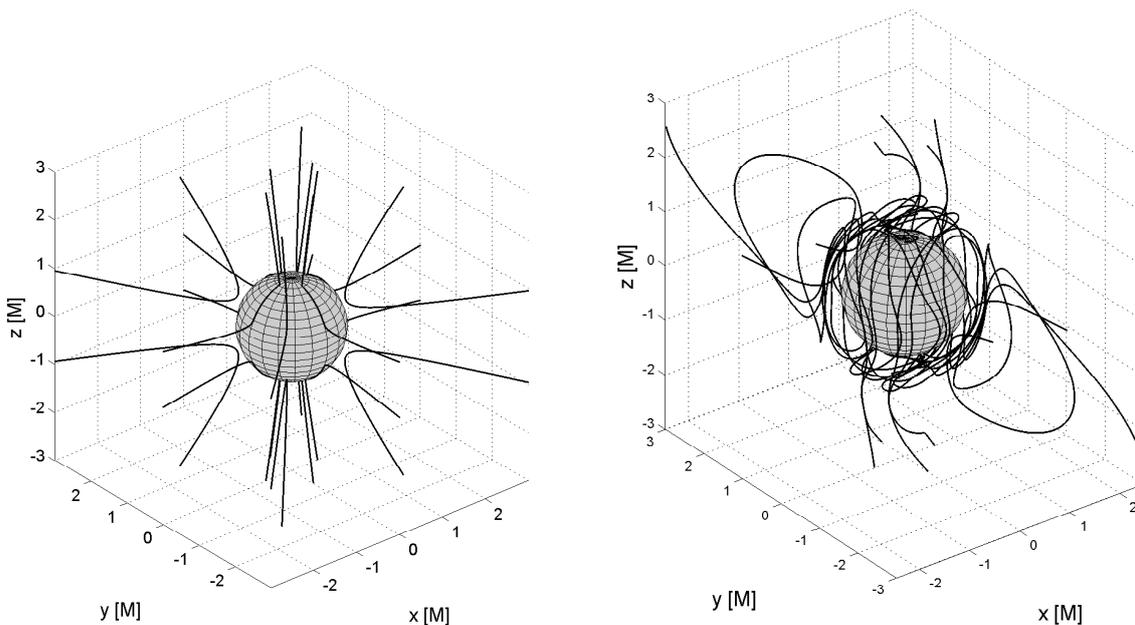
FIGURE 5. Electric field lines (analogous to the magnetic lines) are expelled from the horizon of the non-drifting (stationary) extreme Kerr black hole in the case of an aligned magnetic field ($B_x = 0$) on the background (left panel). However, for the inclined field ($B_x/B_z = 0.3$) the structure of the electric field becomes intricate and some field lines penetrate the horizon (right panel).

By introducing the perpendicular field component, we observe that generally (i) the magnetic field is not expelled any more, and (ii) both the electric field and the magnetic field acquire a tightly layered structure in the narrow zone just above the horizon. This is in agreement with the conclusions in our older papers and also in agreement with the recent discussion by Penna [56, 57]. The structure of the field is surprisingly complex in this region. Self-similar patterns are observed regardless of the choice of the observer proving that the layering is an intrinsic feature of the field rather than a mere observer's effect.

4.2. SEPARATOR RECONNECTION IN THE KERR METRIC WITH A BOOST

In the case of the translational motion of a black hole through the aligned field, we note the complex layering of the field, which we attribute to the transversal

component arising from the Lorentz boost (Figures 4–5). However, for a sufficiently rapid drift motion we observe a new effect emerging: as the layers gradually transform, they give rise to the formation of neutral points of both the electric and the magnetic fields (though not in the same location!). The field structure surrounding such a point is characterised by four distinct domains (bundles of field lines) divided by two separatrices that intersect with each other at the neutral point. Such a topology is known to result from the *separator reconnection*, a mechanism that has been studied in the framework of resistive magnetohydrodynamics, see e.g. [59]. In our electro-vacuum model, however, it arises entirely from the interaction of the strong gravitational field of the rotating BH with the background magnetic field, i.e., the gravitomagnetic effect. Charged matter injected into the magnetic separator site is prone to acceleration by the electric field, since its motion is not affected by the vanishing magnetic field, so the acceleration is very effective.

From the astrophysical viewpoint, we consider the topological changes that the drift causes upon the field structure, especially the formation of the neutral points, as our main result, which demonstrates clearly that the strong gravitation of the rotating Kerr source may itself entangle the uniform magnetic field in a surprisingly complex way. Tentative astrophysical consequences of this still remain under discussion.

We conclude that the gravity of the rotating black hole can act as a trigger for magnetic reconnection. What remains to be further explored is the speed and the overall efficiency of the reconnection process. However, it emerges as a new aspect that the reconnection process can be aided by strong gravity of the rotating black hole where the existence of the ergosphere plays an essential role in shaping the magnetic field lines and in giving rise to the magnetic null points.

5. Motion of particles and fluids

We consider properties of motion (both particles and fluids) in the test regime. The gravitational field has been kept fixed in terms of the prescribed space-time metric (Kerr or Kerr-Newman black hole) and the accreted matter does not contribute to it. Likewise, the imposed magnetic field has its sources in the external currents flowing outside the black hole, and it does not change the metric coefficients. These assumptions are valid in all astrophysical applications under our consideration, because the effects of the black hole fully dominate the gravity in the region of influence.

5.1. Case of electrically charged particles

To provide a mathematical description of the motion of the test matter, we first construct the super-Hamiltonian $\mathcal{H}$ [52],

$$\mathcal{H} = \tfrac{1}{2} g^{\mu\nu}(\pi_\mu - qA_\mu)(\pi_\nu - qA_\nu), \qquad (5)$$
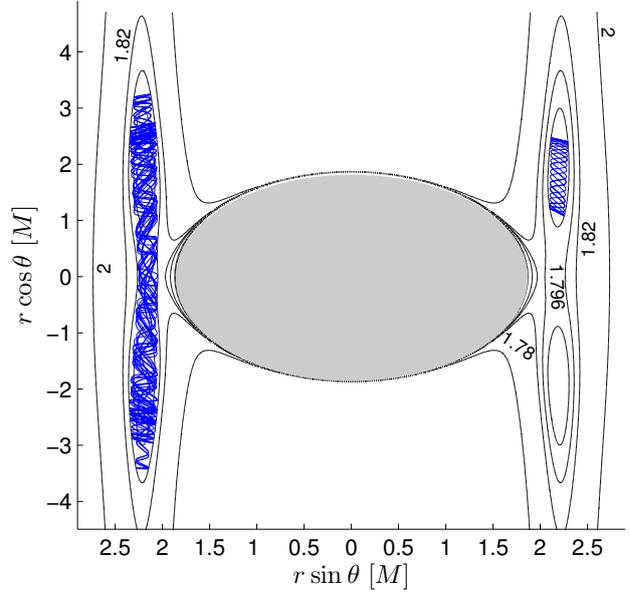
Figure 6. The potential lobes (regions of stable motion) above the horizon of the Kerr black hole (shown as grey surface) immersed in the aligned magnetic field that allows for the off-equatorial orbits of charged particles. Poloidal cut ($\phi = $ const, $t = $ const) across the system is shown. Two different exemplary trajectories are shown; in the left lobe a chaotic orbit is integrated, while in the right lobe an example of a regular (purely off-equatorial) trajectory is shown that differs from the previous one only in the corresponding energy level. All other parameters of the motion have adopted the identical values.

where m and q are the rest mass and the charge of the test particle, π_μ is the generalized (canonical) momentum, $g^{\mu\nu}$ is the metric tensor, and A_μ denotes the vector potential of the electromagnetic field (which is related to the electromagnetic tensor $F_{\mu\nu} = A_{\nu,\mu} - A_{\mu,\nu}$).

Let us note that the same approach can be used to describe the motion of stars when they are treated as point-like particles in the vicinity of a supermassive black hole in galactic nuclei. Again, this is possible as long as the contribution of individual stars to the gravity can be neglected within the close vicinity of the horizon (the domain of black hole gravitational influence). However, let us also remark that these assumptions become violated farther out, at greater distances, where either the fluid torus or the nuclear cluster of stars gains a significant mass compared to the central mass, and so the test regime is no longer a good approximation. Equations of motion can be conveniently written in the Hamiltonian formalism in our analysis. The Hamiltonian equations are given as

$$\frac{dx^\mu}{d\lambda} \equiv p^\mu = \frac{\partial\mathcal{H}}{\partial\pi_\mu}, \quad \frac{d\pi_\mu}{d\lambda} = -\frac{\partial\mathcal{H}}{\partial x^\mu}, \qquad (6)$$

where $\lambda = \tau/m$ is the affine parameter, τ denotes the proper time, and p^μ is the standard kinematical four-momentum for which the first equation reads
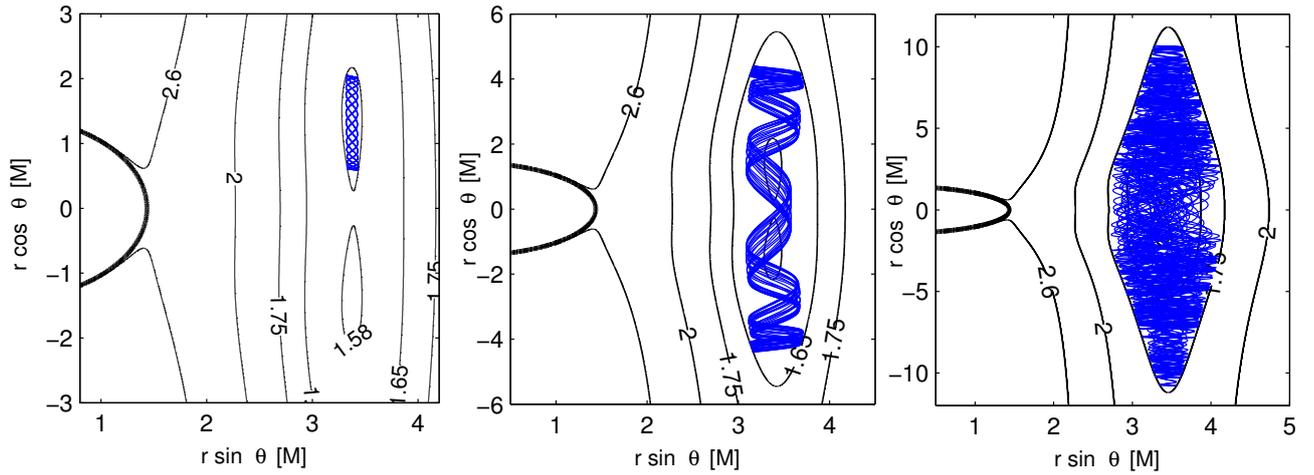
FIGURE 7. A test particle ($\tilde{L} = 6M$, $\tilde{q}B_0 = M^{-1}$ and $\tilde{q}\tilde{Q} = 1$) is launched from the locus of the off-equatorial potential minima $r(0) = 3.68\,M$, $\theta(0) = 1.18$ with $u^r(0) = 0$ and various values of the energy $\tilde{E}$. In the left panel we set $\tilde{E} = 1.58$ and we observe ordered off-equatorial motion. For the energy of $\tilde{E} = 1.65$ we find that cross-equatorial regular motion is relevant (middle panel). Finally in the right panel with $\tilde{E} = 1.75$ we find chaotic motion whose trajectory fills the entire allowed region after the sufficiently long integration time (in accordance with the ergodicity). Spin of the black hole has been set to moderately large value of $a = 0.9\,M$. The event horizon is depicted by the bold line. For different examples and additional discussion [35, 36].
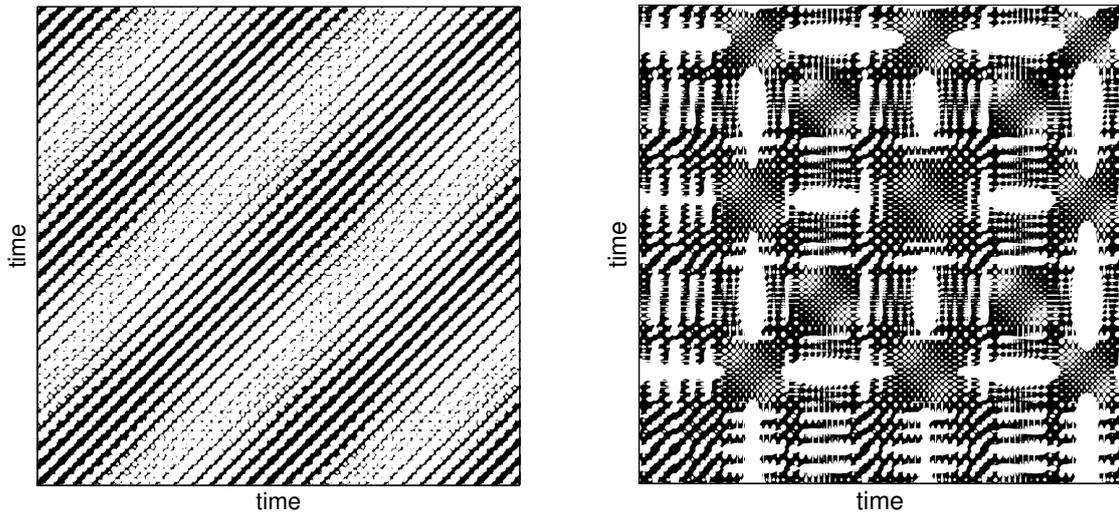
FIGURE 8. Recurrence plots corresponding to the trajectories from Figure 7. The regular orbit leads to the simple diagonal pattern (seen in the left panel), while deterministic chaos manifests itself by the complex structure in the recurrence plot (right panel). Although Recurrence Analysis of the transition to chaos has been applied to various examples of dynamical systems, we have only recently introduced the approach to problems of motion in general relativity. See [36] for a further description of this analysis of the motion in the context of strong gravitational fields. Let us also note that here we exhibit a binary (monochrome) version of recurrence plots, while additional information can in principle be included by colour-coding the temporal information about the maximum Lyapunov exponent, which would add further evidence on how developed the chaos in the system is.

$p^\mu = \pi^\mu - qA^\mu$. In the case of stationary and axially-symmetric systems, we identify two constants of motion, namely, the energy $E \equiv -\pi_t$ and the angular momentum $L \equiv -\pi_\varphi$. The above-given equations are employed to integrate particle trajectories. Quite understandably, in a general situation an analytical solution is not possible, so instead one needs to resort to numerical methods. Because of the possible effect of chaos, it is important to verify the precision and the stability of the numerical scheme. To this en,d we tested several different numerical integrators for their

accuracy, confirming the supremacy of the symplectic solver (see Figure 11).

Let us note that the aspects of chaos in General Relativity (and its alternatives or generalisations) have been actively explored in various context of magnetised black holes and other strongly gravitating systems in very recent literature [4, 21, 24, 25, 46, 48, 62, 64, 69].

There is an obvious caveat that does not allow us to consider a case of perturbed motion in dissipative systems where the energy of the particles is not con-
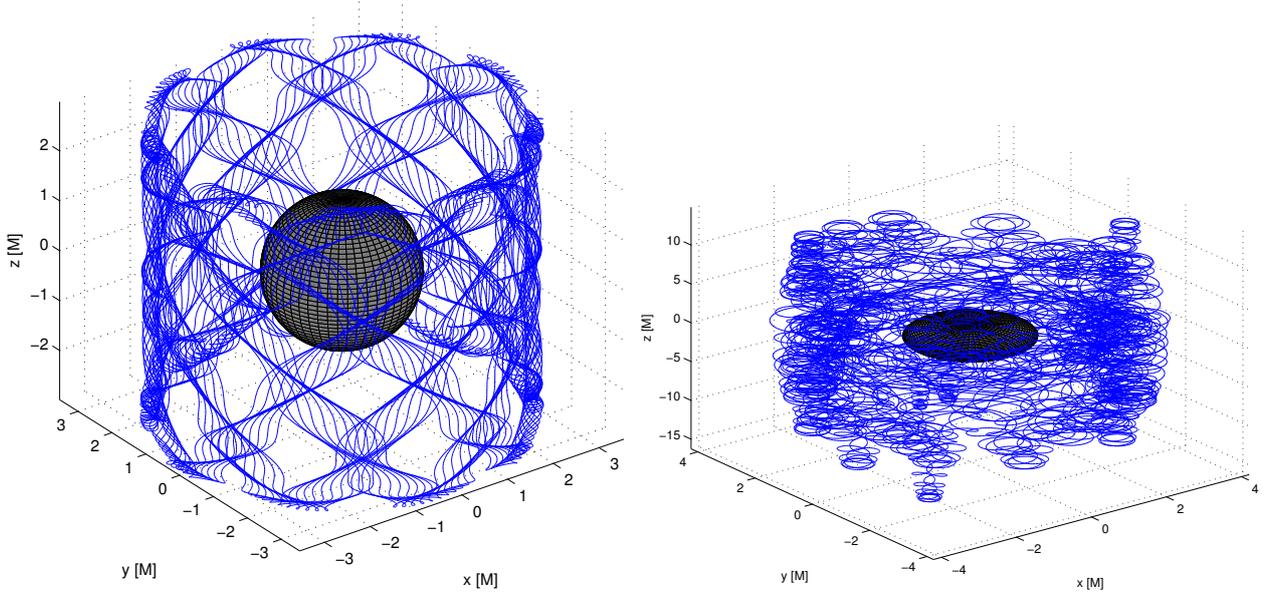
FIGURE 9. Examples of regular versus chaotic trajectories are given. Left panel: a regular trajectory is shown of an electrically charged test particle (parameters $\tilde{q}\tilde{Q} = 1$, $\tilde{L} = 6\,M$ and $\tilde{E} = 1.6$) in the Kerr space-time background metric (spin $a = 0.9\,M$) with the Wald uniform magnetic field ($\tilde{q}B_0 = 1M^{-1}$). The particle is launched initially at $r(0) = 3.68$, $\theta(0) = 1.18\,M$ with zero radial velocity, $u^r(0) = 0$. Right panel: an example of a chaotic trajectory ($\tilde{q}\tilde{Q} = 1$, $\tilde{L} = 6\,M$ and $\tilde{E} = 1.8$) in the Kerr background ($a = 0.9\,M$), again with the Wald magnetic field ($\tilde{q}B_0 = 1M^{-1}$). Now the test particle is launched at $r(0) = 3.68\,M$, $\theta(0) = 1.18$ with $u^r(0) = 0$. See [33] for notation and further details.

served (for example the case of orbital motion when the interaction with the surrounding ambient medium would be taken into account). Let us also note that for general (non-separable) Hamiltonians only implicit symplectic schemes exist. Explicit methods are available for separable Hamiltonians (and for some special forms of non-separable Hamiltonians). There is also a practical inconvenience connected with symplectic methods, namely, their failure to conserve the symplectic structure once the adaptive step-size scheme is employed. However, the accuracy of the symplectic integrator can be further increased by reducing the step-size, although this comes at the expense of computational time. Workarounds have been suggested to combine the benefits of the symplectic scheme and variable-step algorithms.

The effective potential approach offers the most straightforward and effective way to locate off-equatorial orbits. To this end, we derived the form of the effective potential in the following way [35, 36]:

$$V_{\text{eff}} = \frac{-\beta + \sqrt{\beta^2 - 4\alpha\gamma}}{2\alpha}, \qquad (7)$$

where the explicit expression for the three functions is provided in terms of space-time coordinates (t, r, θ, ϕ) and the corresponding contravariant metric terms $g^{\mu\nu}$, namely, $\alpha = -g^{tt}$, $\beta = 2\left[g^{t\varphi}(\tilde{L} - \tilde{q}A_\varphi) - g^{tt}\tilde{q}A_t\right]$, and $\gamma = -g^{\varphi\varphi}\left(\tilde{L} - \tilde{q}A_\varphi\right)^2 - g^{tt}\tilde{q}^2A_t^2 + 2g^{t\varphi}\tilde{q}A_t\left(\tilde{L} - \tilde{q}A_\varphi\right) - 1$. Here we have also introduced the specific angular moment and energy, $\tilde{L} \equiv L/m$, $\tilde{E} \equiv E/m$, and the specific electric charge $\tilde{q} \equiv q/m$.

Let us note that the effective potential method is normally suitable under the assumption of axial symmetry. The extension of this approach to non-axisymmetric situations is not straightforward, but promising alternatives and attempts to generalise the analysis exist in the literature. For example, in [16] the dynamics of charged relativistic particles in the electromagnetic field of a rotating magnetized star with the magnetic axis inclined to the axis of rotation has been studied recently. Clearly, the inclined rotator represents a non-stationary situation where the formalism of a simple effective potential must be modified and treated by numerical approaches. Nonetheless, it also offers a rich area for further investigations, because in this case the system can develop bound or semi-bound regions (valleys), where the charged particles can be trapped.

However, the time-scales related to the misalignment between the black hole symmetry axis and the symmetry of the external magnetic field are quite long, so we can ignore them in the first approximation. Also, we do not embark on generalising the effective potential method in the present work. Instead, we make numerically study of the properties of the motion of electrically charged particles. This gives us some additional freedom to consider both magnetized rotating black holes and compact stars, and to explore both the regular motion and the chaotic motion of the particles (see Figure 9).

To distinguish the qualitatively different types of dynamics, we employed the method of recurrence analysis in the phase space [36]. This approach allows us
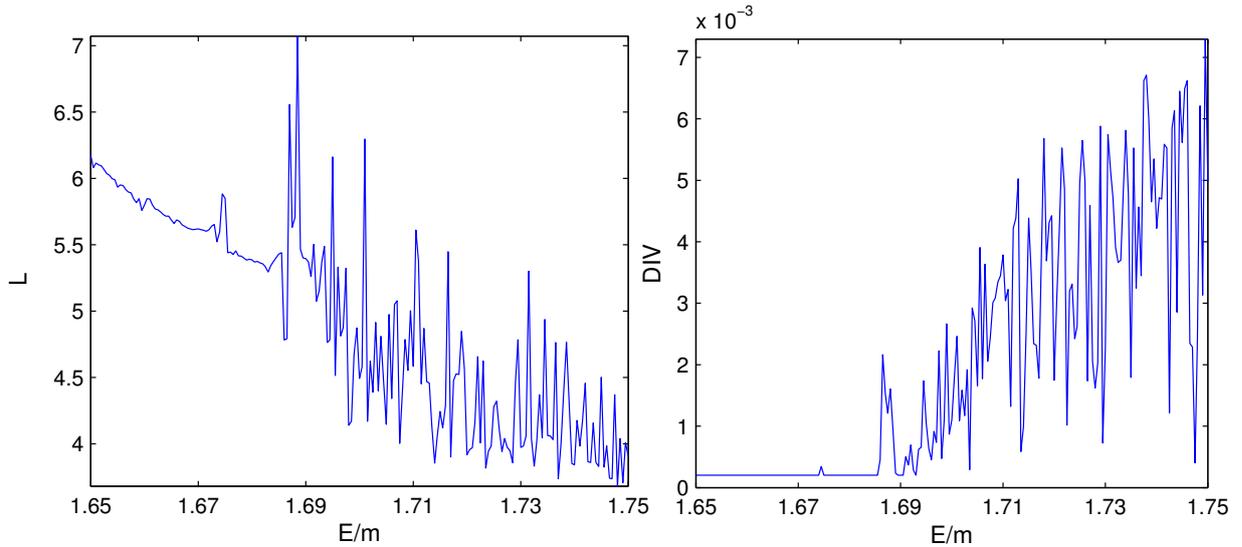
FIGURE 10. Recurrence quantification analysis (RQA) gives us statistical measures of recurrence plots. The average length of the diagonal line L and the inverse of the longest diagonal line DIV are presented here as a function of the specific energy $\tilde{E}$ ($\equiv E/m$); four hundred distinct trajectories were analysed (they differ only in the energy level), as given in Figure 7. A very clear change in behaviour is seen at $\tilde{E} \approx 1.685$, where the trend changes abruptly for both quantities. This property allows us to identify very precisely the moment when chaos sets in.

to characterize the transition to chaos and to quantify the degree of chaoticness of the system. The adopted recurrence analysis has some important advantages in comparison with the more traditional formalism of Poincaré surfaces, although, unlike the latter, Recurrence Plots have not yet been widely used to explore the regime of strong gravity.

Let us note that the primary motivation for these investigations is the question of whether the matter around magnetized compact rotators exhibits the characteristics of chaotic motion, or if instead the system is typically regular. This is relevant from the principal point of view: the motion of test particles near Kerr black holes(electrically neutral) and also Kerr-Newman black holes (electrically charged) is known to be regular, so the question arises about the emergence of chaos in the case of perturbed space times. The problem is interesting also in the context of the motion near neutron stars, where the metric is different from the vacuum black-hole solutions mentioned here. One of the main applications of our considerations concerns the putative envelopes of charged material enshrouding the central body in the form of a fall-back disks and coronae extending above and below the equatorial plane [38, 40, 41]. Let us remind the reader that according to the Carter's seminal work the motion near classical black holes remains regular. However, perturbations are expected to trigger chaos. This includes the electromagnetic effects of external origin, for example the imposed fields that arise due to currents in a surrounding accretion disk.

In summary, in our work we impose a large-scale ordered magnetic field acting on particles in combination with strong gravity, and in such a system we study chaos versus regularity of the motion. Various

aspects of charged particle motion were addressed throughout the PhD dissertation [33], where further references can be found. Let us note that the role of organised (coherent) magnetic fields remains to be understood; indications exist that powerful jets can also be launched also in circumstances when the magnetic field has no large-scale structure. Instead, there is a turbulent field embedded in the accreting material [9]. The turbulent component is thought to arise due to magneto-rotational instability. Magnetic dissipation is then required to sustain further conversion of the Poynting flux into the kinetic energy of the jet or outflow [65].

First of all, we investigated the motion in off-equatorial lobes above the horizon of a rotating black hole (modeled by the Kerr metric endowed by Wald's test magnetic field of external origin), as well as above the surface of a magnetic star (modeled by the Schwarzschild metric with a superposed rotating magnetic dipole). In both cases, we conclude that the motion of the test particles is mainly regular and the same result can be confirmed for a representative number of different trajectories across the wide range of parameters. Note that this includes a range of topological types of the off-equatorial potential wells. It should be emphasised that this result is somewhat unexpected, because the off-equatorial orbits require strong-enough perturbation (in terms of the intensity of the imposed electromagnetic field), to counterbalance the vertical component of the gravitational force.

Further, we investigated the sensitivity of the response of the particle dynamics when the energy level $\tilde{E}$ was gradually raised from the potential minimum up to values that allow cross-equatorial motion (to transit
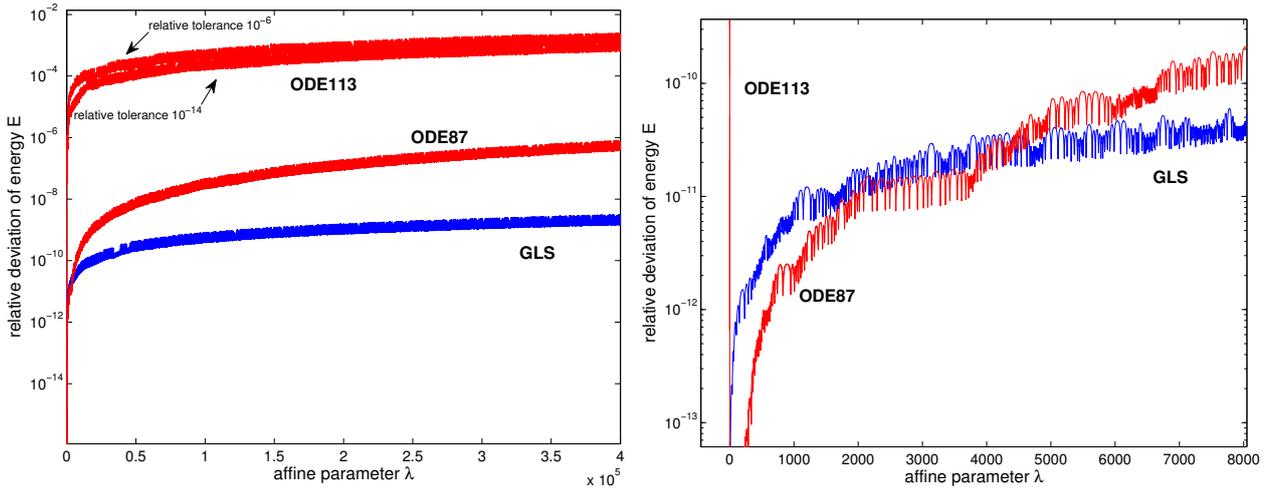
FIGURE 11. A comparison of the global accuracy of several integrators for a chaotic trajectory. For integration times $\lambda \gtrsim 5 \times 10^3$ the symplectic integrator (GLS) dominates in accuracy over other (non-symplectic) schemes with the difference rising steadily. In the left panel we compare the outcome of a multi-step Adams-Bashforth-Moulton solver (ODE113) for two values of the relative tolerance which controls the local error. The explicit Runge-Kutta solver of the 8th order (ODE87) is also presented. The right panel shows the detailed behaviour of the deviation of the energy. We conclude that the symplectic scheme provides the most reliable results.

the equatorial plane the particles need to pass above the local peak of the effective potential which is formed between the two global minima of the off-equatorial lobes). We examined various topological classes of the effective potential and came to the conclusion that cross-equatorial orbits are typically chaotic. However, the complete picture is quite complex, because stable regular orbits may also persist for a certain intermediate energy interval. The classical work of [23] should be recalled in this context. These authors also identified the energy as a trigger for the chaotic motion in their (very simple) system. More recently, the Hénon–Heiles system was revisited in the relativistic context in [66] where the effects of strong gravity are included as in our present work.

Finally, we also addressed the question of the spin dependence of the stability of motion for a Kerr black hole in the Wald field, by which we mean the dependence on the dimensionless angular momentum parameter (relative to the mass), a/M. We noticed that this is a rather subtle problem, but it is a very interesting one, especially because the black hole spin is one of only three free parameters defining classical black holes. The effective potential is by itself sensitive to the spin; we therefore had to link the potential value roughly linearly with the energy $\tilde{E}$ to maintain the potential lobe in a given position. In the end, we did not find a unique indication of the spin dependence of the chaos in the system. Most trajectories exhibited strictly regular behaviour in rather precise agreement with the previous results indicating that the motion in off-equatorial lobes is generally regular. However, in the case of cross-equatorial motion we observed that, for higher spin values, more irregular (non-integrable) properties come into play when compared with the case of small $|a|$ (slow rotation). This

trend can be attributed to simultaneous adjustments of specific energy $\tilde{E}$.

To conclude this part of the discussion, it appears almost impossible to give an unambiguous decision about the spin dependence of the dynamics of the particles. Instead, one has to deal with a complex, interrelated dependence. In the case of a Kerr black hole immersed in a large-scale magnetic field, we found the effect of confinement of particles regularly oscillating around the equatorial plane. The escape of particles from the equatorial plane to large radii above/below the plane is allowed for a given range of initial conditions. The equipotentials do not close. Instead, they form a contour "valley". The escaping trajectories form a narrow, collimated structure parallel to the axis, which to some degree resembles a jet-like path.

5.2. ACCRETION OF MAGNETIZED FLUID TORI ONTO A ROTATING BLACK HOLE

In order to compare different approaches, in this section let us complement our discussion by an alternative scheme that takes magnetohydrodynamical effects into account in the relativistic framework. The MHD scheme would be adequate for a short mean free path (compared with the gravitational radius and the Larmor radius as characteristic length-scales of the system). We will verify that stable toroidal configurations persist. However, the possibility of non equatorial structures is less apparent unless the fluid is allowed to possess a non-vanishing electric charge [38, 39].

The magnetized ideal fluid can be described by the energy-momentum tensor [5, 20]

$$T^{\mu\nu} = \left(w + b^2\right) u^\mu u^\nu + P_{\mathrm{g}}\, g^{\mu\nu} - b^\mu b^\nu, \qquad (8)$$

where w is the specific enthalpy, P_g is the gas pressure, and b^μ is the projection of the magnetic field vector ($b^2 = b^\mu b_\mu$), all of them functions of spatial coordinates. From the energy-momentum tensor conservation, $T^{\mu\nu}_{;\nu} = 0$, it follows, for a perfect fluid in permanent rotation:

$$\ln|u_t| - \ln|u_{t_{\text{in}}}| + \int_0^{P_g} w^{-1}\, dP$$
$$- \int_0^l (1 - \Omega l)^{-1}\Omega\, dl + \int_0^{\tilde{P}_m} \tilde{w}^{-1}\, d\tilde{P} = 0,$$

where u_t is the covariant component of the four-velocity (subscript 'in' refers to the inner edge of the torus), $\Omega = u^\varphi/u^t$ is the angular velocity and $l = -u_\varphi/u_t$ is the angular momentum density [1, 2]. Assuming the polytropic equation of state and the rotation law of the fluid, the torus structure can be integrated to obtain the structure of equipotential surfaces of the figures of equilibrium.

We assume that the above-described initial stationary state is perturbed out of equilibrium. This leads to the capture of a small amount of material by the black hole, which increases the black-hole mass, and so accretion occurs. The authors of [3] argued that tori with radially increasing angular momentum density are more stable. To check on this assertion, our algorithm for the numerical experiment proceeds as follows [20]. In the initial step the mass of the black hole was increased by a small amount, typically by a few percent. After each time-step δt, an elementary parcel of mass δM and angular momentum $\delta L = l(R_{\text{in}})\,\delta M$ are accreted across the horizon, $r = r_+ \equiv [1 + \sqrt{1 - a^2}]\,GM/c^2$. The mass increase δM is computed as the difference of the mass of the torus $M_d = \int_V \rho\, d\mathcal{V}$ at t and $t + \delta t$, where $d\mathcal{V} = u^t\sqrt{-g}\, d^3x$ is taken over the spatial volume occupied by the torus. The corresponding elementary spin increase is $\delta a = l\,\delta M/(M + \delta M)$. Therefore, at each step of the simulation we update the model parameters by corresponding low values of the mass and angular momentum changes: $M \rightarrow M + \delta M$, $a \rightarrow a + \delta a$. The inner cusp moves accordingly.

We explored the dependence of the torus mass on time for different values of the ratio between thermodynamical and magnetic pressure (plasma parameter), $\beta_p \equiv P_g/P_m$, for a torus with radially increasing distribution of the angular momentum, $l(R) = l_{K,\, R=R_{\text{in}}}[1 + \epsilon(R - R_{\text{in}})]^q$ with $q > 0$, $0 < \epsilon \ll 1$. This means that the reference level of the angular momentum density is set to $l = \text{const} = l_K(R_{\text{in}})$, motivated by the standard theory of thick accretion discs, where the constant value is the limit relevant for stability.

By numerical integration of the mass transfer, we verified as our main result that a radially growing profile helps to stabilise the configuration. The amount of accreted mass is generally larger for smaller β_p and the overall gradually decreasing trend is superposed with fast oscillations. After the initial drop in the mass of the torus (due to the magnitude of the initial perturbation, $\delta M \simeq 0.01M$), phases of enhanced accretion change with phases of diminished or zero accretion.

6. OPEN QUESTIONS AND PROSPECTS

In the following part of the paper, we will present our *to-do list* comprising open questions and various issues that have arisen in previous studies of electromagnetic fields and charged particle dynamics. Most importantly, we want to combine two major topics that were presented separately in [33]. Namely, we plan to investigate the motion of an electrically charged (ionized) particle governed by the generalized *oblique and drifting* electromagnetic fields. In addition, we will go through several rather technical issues related closely to this problem, in particular, the recurrence analysis of chaotic trajectories and the off-equatorial orbits around magnetised black holes. Finally, we wish to complement the discussion within the particle framework with a complementary methodology for general relativistic MHD, as mentioned in the previous subsection.

However, let us remind the reader that we still adopt the approximation of the test electromagnetic fields and the test fluid moving through the prescribed spacetime metric. The gravitational field is therefore still described by the Kerr metric. The parameters of the Kerr metric (namely, the mass and the spin) can evolve as the material is transferred onto the black hole. However, the form of the metric is assumed to stay the same.

6.1. PARTICLES IN A HIGHLY DILUTED CORONA OF A BLACK HOLE ACCESSION DISK

We will extend our former axisymmetric model by considering oblique (misaligned with the rotation axis) magnetic fields in which the central body may be uniformly drifting in a general direction [34, 35, 53]. The structure of the electromagnetic field is profoundly enriched and we suppose that similarly the dynamics of the particles will become considerably more complex. We plan to discuss the impact of new parameters on the off-equatorial stable orbits and to investigate how they affect the dynamic motion regime. We will try to identify a possible trigger of chaotic dynamics among new parameters. In addition to standard methods, recurrence analysis will be employed since it proved useful in our previous work.

We also plan to further elaborate ideas concerning frequency analysis of the off-equatorial orbits. We have seen that the fragmented curves that we observed in the Poincaré surfaces of the section corresponding with the trajectories bound in the closed equatorial lobes may be identified with the Birkhoff chains of islands of stability. Such a resonance chain is characterized by a single value of the rotation number, which is in principle detectable in terms of spectral analysis

of the observed signal. The presence of the Birkhoff chains allows us to discriminate between perturbed and regular systems, so this offers very interesting and challenging prospects for future research. Moreover the position and the width of these chains reflect other properties of the system. A detailed discussion of this approach applied to a different type of system may be found in [47].

However, in our analysis of off-equatorial trajectories we also observed more complicated structures in the surfaces of the section which do not allow for a straightforward evaluation of the rotation number, or of the ratio of the fundamental frequencies. We therefore intend to adjust the method for application to our scenario, and to infer the possible observational consequences for the system of a gaseous corona. An obvious caveat and a complication arises from the fact that the individual particles contribute just a tiny fraction of the total outgoing signal from the system, so it appears difficult to disentangle many different contributions unless some coherent characteristic can be defined.

In the integrable system the trajectories in the phase space reside on the surface of tori characterized by the values of integrals of motion which determine the characteristic frequencies of the orbit. The fundamental frequencies in the axisymmetric system (here we do not consider oblique or drifting fields) are the frequencies of radial and latitudinal motion. Once the system is slightly perturbed (by the magnetic field in our model) the tori characterized by the irrational ratio of frequencies survive, which is assured by the KAM theorem.

However, the Poincaré–Birkhoff theorem tells us that resonant tori with the rational frequency ratio must disintegrate into a chain of islands when the system is perturbed. Such resonant chains are in principle detectable in terms of spectral analysis of the observed signal. Presence of the Birkhoff chains allows us to discriminate between perturbed and regular systems. Moreover the position and the width of the chains reflects other properties of the system.

6.2. Magnetic shift of the ISCO

The position of the inner edge of the accretion disk is usually identified with the marginally stable geodesic orbit $r_{\rm ms}$ (also referred to as the Innermost Stable Circular Orbit – ISCO) the position of which is uniquely determined by the value of the black hole spin a [8].

A common approach to the measurement of black-hole spin is based on this relation; in other words, the location of the inner edge $r = r_{\rm ms}(a)$ is inferred by a spectrum fitting method, and then it is employed to evaluate the spin a [50]. In this context, we raise the question whether the presence of the magnetic field may change the position of ISCO noticeably. Recently, a similar problem was addressed by [6] for the case of a Schwarzschild source endowed with the dipole magnetic field. An introductory account of

the influence of the uniform magnetic field aligned with the symmetry axis of a Kerr black hole was provided by [58]. We will discuss in detail the effect of the oblique uniform magnetic field around the Kerr source on the marginally stable orbit.

6.3. Application to Lyapunov spectra

Lyapunov characteristic exponents (LCEs) are the basic indicators of chaos which capture the divergent features of chaotic orbits straightforwardly. The classical non-covariant definition of LCEs, however, meets difficulties when applied to curved spacetimes [30, 46] for two reasons: firstly, there is the possible occurrence of singularities, and secondly there is the complication of coordinate transformations that need to be taken into account.

Recently, [63] proposed a novel geometrical approach to the computation of the Lyapunov spectra which completely avoids the conventional method for solving the variational equations to obtain the Lyapunov vectors which are periodically Gram-Schmidt orthonormalized along the flow. This new algorithm adopts a covariant formulation, so it seems to be highly suitable for application in a general-relativistic framework. We plan to implement this method when inspecting the dynamics of charged particles, which should be beneficial for proving the new method fruitful (Kopáček et al., work in progress).

6.4. Magnetized fluid accretion tori

Under certain conditions, the material of a star in a binary system can be transferred to another component. Such a situation arises when one of the two stars expands and fills up its Roche lobe, or when a star loses material due to a strong stellar wind. In this case, neither the approximation of spherical accretion ($v_\phi = v_\theta = 0$, $v_r \neq 0$) nor the Bondi-Hoyle limit of accretion onto a moving object ($v_\phi = 0$, $v_z \neq 0$) is appropriate. Disk-like hydrodynamical accretion appears as the most relevant type of accretion of material with nonvanishing angular momentum in astrophysics. Stability of the configuration and angular momentum transport are of crucial importance in the accretion theory.

In the context of MHD simulations of relativistic fluid tori, one of open questions that needs to be explored further concerns the potential role of large-scale (organised) magnetic fields that may thread some regions of the flow. In particular, they may penetrate the corona. These organised fields are thought to help the formation of jets and outflows, and they may even suppress turbulent motions, but this is clearly a complex problem that we do not attempt to discuss here. In our simulations we have started with a purely toroidal field for which the well-known analytical solution [31] allows us to formulate simplified models. By employing the numerical approach we can evolve the initial configuration to more complex systems where

the mutual interaction between the magnetic fields and fluid motions induces the poloidal component.

The gravitational effects on oblique magnetic fields near a rotating black hole have been explored in [28, 29], where the conclusions summarised in this paper can be found in further detail. For more details concerning various aspects of the onset of chaos, namely, the context of transition from regular to chaotic motion and the use of Recurrence Analysis to recognise the motion characteristics in the strong-gravity regime, we invite the reader to study our recent papers [33, 35]. For further details about evolving the organised magnetic fields and fluids during the accretion process, within the framework of the relativistic MHD limit, see [19, 20].

References

[1] Abramowicz, M. A., & Fragile, P. C.,: Foundations of Black Hole Accretion Disk Theory, *Living Rev. Relativity*, 16, 1, 2013, DOI:10.12942/lrr-2013-1

[2] Abramowicz, M. A., Jaroszyński, M., & Sikora, M.: Relativistic, accreting disks, *Astronomy & Astrophysics*, 63, 221, 1978

[3] Abramowicz, M. A., Karas, V., & Lanza A.: On the runaway instability of relativistic tori, *Astronomy & Astrophysics*, 331, 1143, 1998

[4] Al Zahrani, A. M., Frolov, V. P., & Shoom, A. A.: Critical escape velocity for a charged particle moving around a weakly magnetized Schwarzschild black hole, *Physical Review D*, 87, id. 084043, 2013, DOI:10.1103/PhysRevD.87.084043

[5] Anile, A. M.: Relativistic Fluids and Magneto-Fluids (Cambridge University Press: Cambridge), 1989

[6] Bakala, P., Šrámková, E., Stuchlík, Z., & Török, G.: On magnetic-field-induced non-geodesic corrections to relativistic orbital and epicyclic frequencies, *Classical and Quantum Gravity*, 27, 045001, 2010, DOI:10.1088/0264-9381/27/4/045001

[7] Balbus S. A.: On magnetothermal instability in cluster cooling flows, *The Astrophysical Journal*, 372, 25, 1991, DOI:10.1086/169951

[8] Bardeen, J. M., Press, W. H., & Teukolsky, S. A.: Rotating black holes: locally nonrotating frames, energy extraction, and scalar synchrotron radiation, *The Astrophysical Journal*, 178, 347-370, 1972, DOI:10.1086/151796

[9] Begelman, M. C.: Accreting black holes, in Astrophysics and Cosmology, proceedings of the 26th Solvay Conference on Physics, eds. R. Blandford and A. Sevrin (World Scientific) 2014, in press (arXiv:1410.8132)

[10] Begelman, M. C., Blandford, R. D., & Rees, M. J.: Theory of extragalactic radio sources, *Reviews of Modern Physics*, 56, 255, 1984, DOI:10.1103/RevModPhys.56.255

[11] Bičák, J., & Dvořák, L.: Stationary electromagnetic fields around black holes. III. General solutions and the fields of current loops near the Reissner-Nordström black hole, *Physical Review D*, 22, 2933-2940, 1980, DOI:10.1103/PhysRevD.22.2933

[12] Bičák, J., Ledvinka, T., & Karas, V.: Black holes and magnetic fields, in Black Holes from Stars to Galaxies – Across the Range of Masses, in Proc. IAU Symposium 238, eds. V. Karas & G. Matt (Cambridge University Press: Cambridge), pp.139-144, 2007, DOI:10.1017/S1743921307004851

[13] Carter, B.: Global structure of the Kerr family of gravitational fields, *Physical Review*, 174, 1559-1571, 1968, DOI:10.1103/PhysRev.174.1559

[14] Casares, J.: Observational evidence for stellar-mass black holes, in Black Holes from Stars to Galaxies – Across the Range of Masses, in Proc. IAU Symposium 238, eds. V. Karas & G. Matt (Cambridge University Press: Cambridge), pp. 3-12, 2007, DOI:10.1017/S1743921307004590

[15] Done, C.: Galactic black hole binary systems, *Advances in Space Research*, 28, 255-265, 2001, DOI:10.1016/S0273-1177(01)00404-5

[16] Epp, V., & Masterova, M. A.: Effective potential energy for relativistic particles in the field of inclined rotating magnetized sphere, *Astrophysics and Space Science*, 353, 473-483, 2014, DOI:10.1007/s10509-014-2066-9

[17] Falcke, H., & Biermann, P. L.: The jet-disk symbiosis I. radio to X-ray emission models for quasars, *Astronomy and Astrophysics*, 293, 665-682, 1995

[18] Ferrière, K.: The interstellar magnetic field near the Galactic center, *Astronomische Nachrichten*, 331, 27-33, 2010, DOI:10.1002/asna.200911253

[19] Hamerský: in preparation, Ph.D. Thesis (Charles University: Prague), 2015

[20] Hamerský, J., & Karas, V.: Effect of the toroidal magnetic field on the runaway instability of relativistic tori, *Astronomy & Astrophysics*, 555, A32, 2013, DOI:10.1051/0004-6361/201321500

[21] Han, Wenbiao: Chaos and dynamics of spinning particles in Kerr spacetime, *General Relativity and Gravitation*, 40, 1831-1847, 2008, DOI:10.1007/s10714-007-0598-9

[22] Hawley J. F., & Krolik, J. H.: Magnetically driven jets in the Kerr metric, *The Astrophysical Journal*, 641, 103-116, 2006, DOI:10.1086/500385

[23] Hénon, M., & Heiles, C.: The applicability of the third integral of motion: Some numerical experiments, *Astronomical Journal*, 69, 73, 1964, DOI:10.1086/109234

[24] Huang, Qi-Hong, Chen, Ju-Hua, & Wang, Yong-Jiu: Chaotic motion of a charged particle around a weakly magnetized Schwarzschild black hole containing cosmic string, *Chinese Physics Letters*, 31, id. 060402, 2014, DOI:10.1088/0256-307X/31/6/060402

[25] Igata, T., Ishihara, H., & Takamori, Y.: Chaos in geodesic motion around a black ring, *Physical Review D*, 83, id. 047501, 2011, DOI:10.1103/PhysRevD.83.047501

[26] Junor, W., Biretta, J. A., & Livio, M.: Formation of the radio jet in M87 at 100 Schwarzschild radii from the central black hole, *Nature*, 401, 491, 1999, DOI:10.1038/44780

[27] Karas, V., & Kopáček, O.: Magnetic layers and neutral points near a rotating black hole, *Classical and Quantum Gravity*, 26, 025004, 2009, DOI:10.1088/0264-9381/26/2/025004

[28] Karas, V., Kopáček, O., & Kunneriath, D.: Influence of frame-dragging on magnetic null points near rotating black holes, *Classical and Quantum Gravity*, 29, 035010, 2012, DOI:10.1088/0264-9381/29/3/035010

[29] Karas, V., Kopáček, O., & Kunneriath, D.: Magnetic neutral points and electric lines of force in strong gravity of a rotating black hole, *International Journal of Astronomy and Astrophysics*, 3, 18-24, 2013, DOI:10.4236/ijaa.2013.33A003

[30] Karas, V., & Vokrouhlický, D.: Chaotic motion of test particles in the Ernst space-time, *General Relativity & Gravitation*, 24, 729-743, 1992, DOI:10.1007/BF00760079

[31] Komissarov, S. S.: Magnetized tori around Kerr black holes: analytic solutions with a toroidal magnetic field, *Monthly Notices of the Royal Astronomical Society*, 368, 993-1000, 2006, DOI:10.1111/j.1365-2966.2006.10183.x

[32] Kopáček, O.: Asymptotically uniform electromagnetic test fields around a drifting Kerr black hole, in WDS'08 Proceedings: Part III – Physics, eds. J. Šafránková & J. Pavlů (Matfyzpress: Prague), pp. 198-203, 2008

[33] Kopáček, O.: Transition from Regular to Chaotic Motion in Black Hole Magnetospheres, Ph.D. Thesis (Charles University: Prague), 2011

[34] Kopáček, O., & Karas, V.: Electro-magnetic fields around a drifting Kerr black hole, in Proc. of IAU Symposium 259: Cosmic Magnetic Fields: From Planets, to Stars and Galaxies, eds. K. G. Strassmeier, A. G. Kosovichev & J. E. Beckman, Cambridge University Press, Cambridge, pp. 127-128, 2009

[35] Kopáček, O., & Karas, V.: Inducing chaos by breaking axial symmetry in black hole magnetosphere, *The Astrophysical Journal*, 787, 117, 2014, DOI:10.1088/0004-637X/787/1/1

[36] Kopáček, O., Karas, V., Kovář, J., & Stuchlík, Z.: Transition from regular to chaotic circulation in magnetized coronae near compact objects, *The Astrophysical Journal*, 722, 1240-1259, 2010a, DOI:10.1088/0004-637X/722/2/1240

[37] Kopáček, O., Kovář, J., Karas, V., & Stuchlík, Z.: Recurrence plots and chaotic motion around Kerr black hole, in Proc. of Conference Mathematics and Astronomy: A Joint Long Journey, eds. M. de León, D. M. de Diego, & R. M. Ros (Springer: Berlin), vol. 1283, pp. 278-287, 2010b, DOI:10.1063/1.3506071

[38] Kovář, J., Kopáček, O., Karas, V., & Stuchlík, Z.: Off-equatorial orbits in strong gravitational fields near compact objects – II: halo motion around magnetic compact stars and magnetized black holes, *Classical and Quantum Gravity*, 27, 135006, 2010, DOI:10.1088/0264-9381/27/13/135006

[39] Kovář, J., Slaný, Cremaschini, C., Stuchlík, Z., Karas, V., & Trova, A.: Electrically charged matter in rigid rotation around magnetized black hole, *Physical Review D*, 90, 044029, 2014, DOI:10.1103/PhysRevD.90.044029

[40] Kovář, J., Slaný, P., Stuchlík, Z., Karas, V., Cremaschini, C., & Miller, J. C.: Role of electric charge in shaping equilibrium configurations of fluid tori encircling black holes, *Physical Review D*, 84, 084002, 2011, DOI:10.1103/PhysRevD.84.084002

[41] Kovář, J., Stuchlík, Z., & Karas, V.: Off-equatorial orbits in strong gravitational fields near compact objects, *Classical and Quantum Gravity*, 25, 095011, 2008, DOI:10.1088/0264-9381/25/9/095011

[42] Krolik, J. H. & Hawley, J. F.: General Relativistic MHD Jets, *Lecture Notes in Physics*, 794, 265, 2010, DOI:10.1007/978-3-540-76937-8_10

[43] Kunneriath, D., Eckart, A., Vogel, S. N., Teuben, P., Mužić, K.: The Galactic centre mini-spiral in the mm-regime, *Astronomy & Astrophysics*, 538, A127, 2012, DOI:10.1051/0004-6361/201117676

[44] LaRosa, T. N., Nord, M. E., Lazio, T. J. W., & Kassim, N. E.: New nonthermal filaments at the Galactic Center: are they tracing a globally ordered magnetic field?, *The Astrophysical Journal*, 607, 302-308, 2004, DOI:10.1086/383233

[45] Lipunov, M. M., Börner, G., & Wadhwa, R. S.: Astrophysics of Neutron Stars, Astronomy and Astrophysics Library (Springer: New York), 1992

[46] Lukes-Gerakopoulos, G.: Adjusting chaotic indicators to curved spacetimes, *Physical Review D*, 89, 043002, 2014, DOI:10.1103/PhysRevD.89.043002

[47] Lukes-Gerakopoulos, G., Apostolatos, T. A., & Contopoulos, G.: Observable signature of a background deviating from the Kerr metric, *Physical Review D*, 81, 124005, 2010, DOI:10.1103/PhysRevD.81.124005

[48] Ma, Da-Zhu, Wu, Jian-Pin, & Zhang, Jifang: Chaos from the ring string in a Gauss-Bonnet black hole in AdS5 space, *Physical Review D*, 89, id.086011, 2014, DOI:10.1103/PhysRevD.89.086011

[49] Marwan, N., Carmen Romano, M., Thiel, M., & Kurths, J.: Recurrence plots for the analysis of complex systems, *Physics Reports*, 438, 237-329, 2007, DOI:10.1016/j.physrep.2006.11.001

[50] McClintock, J. E., Narayan, R., Davis, S. W., Gou, L., Kulkarni, A., Orosz, J. A., Penna, R. F., Remillard, R. A., & Steiner, J. F.: Measuring the spins of accreting black holes, *Classical and Quantum Gravity*, 28, 114009, 2011, DOI:10.1088/0264-9381/28/11/114009

[51] Mestel, L.,: Stellar Magnetism (Clarendon Press: Oxford), 1999

[52] Misner, C. W., Thorne, K. S., & Wheeler, J. A.: Gravitation (Freeman: San Francisco), 1973

[53] Morozova, V. S., Rezzolla, L., & Ahmedov, B. J.: Nonsingular electrodynamics of a rotating black hole moving in an asymptotically uniform magnetic test field, *Physical Review D*, 89, 104030, 2014, DOI:10.1103/PhysRevD.89.104030

[54] Morris, M.: The magnetic field in the inner 70 parsecs of the Milky Way, in Proc. of IAU Symposium 140: Galactic and intergalactic magnetic fields, eds. R. Beck, R. Wielebinski & P. P. Kronberg (Kluwer Academic Publishers: Dordrecht), pp. 361-368, 1990

[55] Nord, M. E., Lazio, T. J. W., Kassim, N. E., Hyman, S. D., LaRosa, T. N., Brogan, C. L., & Duric, N: High-resolution, wide-field imaging of the Galactic Center region at 330 MHz, *The Astronomical Journal*, 128, 1646-1670, 2004, DOI:10.1086/424001

[56] Penna, R. F.: Black hole Meissner effect and Blandford-Znajek jets, *Physical Review D*, 89, 104057, 2014a, DOI:10.1103/PhysRevD.89.104057

[57] Penna, R. F.: Black hole Meissner effect and entanglement, *Physical Review D*, 90, 043003, 2014b, DOI:10.1103/PhysRevD.90.043003

[58] Prasanna, A. R., & Vishveshwara, V.: Charged particle motion in an electromagnetic field on Kerr background geometry, *Pramana*, 11, 359-377, 1978, DOI:10.1007/BF02848160

[59] Priest, E., & Forbes, T.: Magnetic Reconnection (Cambridge University Press: Cambridge), 2000

[60] Punsly, B.: Black Hole Gravitohydrodynamics (Springer: Berlin), 2008

[61] Rezzolla, L., Giacomazzo, B., Baiotti, L., Granot, J., Kouveliotou, C., & Aloy, M. A.: The missing link: merging neutron stars naturally produce jet-like structures and can power short gamma-ray bursts, *The Astrophysical Journal Letters*, 732, L6, 2011, DOI:10.1088/2041-8205/732/1/L6

[62] Semerák, O., & Suková, P.: Free motion around black holes with discs or rings: between integrability and chaos – I, *Monthly Notices of the Royal Astronomical Society*, 404, 545-574, 2010, DOI:10.1111/j.1365-2966.2009.16003.x

[63] Stachowiak, T., & Szydlowski, M.: A differential algorithm for the Lyapunov spectrum, *Physica D: Nonlinear Phenomena*, 240, 1221-1227, 2011, DOI:10.1016/j.physd.2011.04.007

[64] Takahashi, M., & Koyama, H.: Chaotic motion of charged particles in an electromagnetic field surrounding a rotating black hole, *The Astrophysical Journal*, 693, 472-485, 2009, DOI:10.1088/0004-637X/693/1/472

[65] Tchekhovskoy, A., McKinney, J. C., & Narayan, R.: Efficiency of magnetic to kinetic energy conversion in a monopole magnetosphere, *The Astrophysical Journal*, 699, 1789-1808, 2009, DOI:10.1088/0004-637X/699/2/1789

[66] Vieira, W. M., & Letelier, P. S.: Chaos around a Hénon-Heiles-Inspired exact perturbation of a black hole, *Physical Review Letters*, 76, 1409-1412, 1996, DOI:10.1103/PhysRevLett.76.1409

[67] Wald, R. M.: Black hole in a uniform magnetic field, *Physical Review D*, 6, 1680-1685, 1974, DOI:10.1103/PhysRevD.10.1680

[68] Wu, X., & Huang, T. Y.: Computation of Lyapunov exponents in general relativity, *Physics Letters A*, 313, 77-81, 2003, DOI:10.1016/S0375-9601(03)00720-5

[69] Yazadjiev, S. S.: Thermodynamics of rotating charged dilaton black holes in an external magnetic field, *Physics Letters B*, 723, 411-416, 2013, DOI:10.1016/j.physletb.2013.05.028